

Noncollinear double quasi phase matching in one-dimensional poled crystals

Tal Ellenbogen and Ady Arie

Department of Physical Electronics, Faculty of Engineering, Tel-Aviv University, Tel-Aviv 69978, Israel

Solomon M. Saitiel

Faculty of Physics, University of Sofia, 5 J. Bourchier Boulevard, 1164 Sofia, Bulgaria

Received August 29, 2006; revised October 6, 2006; accepted October 20, 2006;
posted October 24, 2006 (Doc. ID 74428); published January 12, 2007

We demonstrate simultaneous phase matching of two different nonlinear processes, using a noncollinear interaction in periodically poled crystal with single grating. The noncollinear scheme provides phase-matching solutions over continuous regions of the optical spectrum and can be used for multiple-harmonic generation as well as all-optical effects. We have demonstrated experimentally third-harmonic generation of a 3 μm pump wavelength in a noncollinear configuration using a periodically poled LiNbO₃ crystal. We observed, in good agreement with theoretical calculation, very broad spectral and thermal acceptance bandwidths, as well as a relatively narrow angular bandwidth. © 2007 Optical Society of America
OCIS codes: 190.2620, 190.4160, 190.4360.

Quasi phase matching (QPM) by periodic one-dimensional (1D) modulation of the nonlinear coefficient makes it possible to phase match a single nonlinear interaction.¹ In some cases several nonlinear interactions should be phase matched, e.g., for multiple-harmonic generation or all-optical cascading effects.² Simultaneous phase matching of several processes can be done by 1D quasi-periodic modulation,^{3,4} by periodic phase reversal of the periodic pattern,⁵ and by using periodic⁶ or quasi-periodic⁷ two-dimensional (2D) modulation of the material. These structures are more complex to design and produce than the 1D periodic structure. In this Letter we show that simultaneous phase matching is also possible by using this simple structure, provided that noncollinear interactions are used.

Periodic structures have been used previously by Pfister *et al.*⁸ for simultaneous generation of the second-harmonic (SH) and third-harmonic (TH) in a collinear interaction by relying on coincidence occurrence of two phase-matching conditions at integer multiples of $2\pi/\Lambda$, where Λ is the QPM period. Hence this method is useful for a limited set of discrete wavelengths that satisfy this condition. Although noncollinear interactions have been considered,⁹ the main emphasis was on collinear interactions.

Using a noncollinear interaction provides another degree of freedom that can be used, together with the QPM period, for simultaneously phase matching two different interactions. Furthermore, in a noncollinear configuration, the double-phase-matching (DPM) condition can be satisfied over a broad spectral range.² In 2D periodically poled structures the noncollinearity is always present, and this type of poled structure allows simultaneous generation of SH and TH⁶; however, the 1D poled structure is easier to produce and is commercially available. Our purpose in this work is to explore the possibility of DPM in 1D poled crystal.

The inset in Fig. 1 shows the vector scheme for noncollinear DPM TH generation (THG) interaction

with extraordinary polarized waves. In this case the two cascading processes are governed by the strongest second-order component of LiNbO₃, d_{33} . To find the configuration that satisfies both phase-matching conditions, one has to solve a set of two vector-sum equations for the two different processes. For the DPM THG example, the SH process is phase matched by the reciprocal lattice vector $G_{m_1} = 2\pi m_1/\Lambda$, and the sum frequency of the fundamental and the SH is phase matched by $G_{m_2} = 2\pi m_2/\Lambda$. Using the vector scheme illustrated in the inset of Fig. 1, it is easy to see that the equivalent system of equations is $k_2^2 - 4k_1^2 = G_{m_1}^2 - 4k_1 G_{m_1} \cos \varphi$ and $k_3^2 - 9k_1^2 = (G_{m_1} + G_{m_2})^2 - 6k_1(G_{m_1} + G_{m_2}) \cos \varphi$, where k_1 , k_2 , and k_3 are the wave vectors for ω , 2ω , and 3ω , respectively. The solution of this system for the period of the QPM grating for DPM THG is given by

$$\Lambda = 2\pi \left[\frac{m_1(m_1 + m_2)(2m_2 - m_1)}{2m_1(k_3^2 - 9k_1^2) - 3(m_1 + m_2)(k_2^2 - 4k_1^2)} \right]^{1/2}. \quad (1)$$

The angle φ is found by substituting the period solution at any of the two vector-sum equations. Figure 1

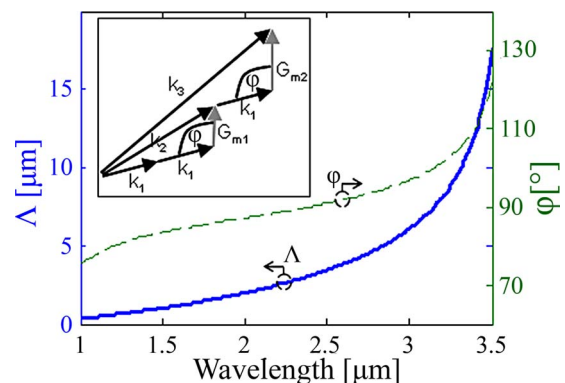


Fig. 1. (Color online) Period and angle solutions for 1–3.5 μm pump wavelengths for THG by the noncollinear DPM process using PPLN. Inset, QPM vector scheme for THG by the noncollinear DPM process.

shows the poling period Λ and the angle φ between the reciprocal lattice vector and the pump direction for $m_1=m_2=1$. It is shown that for every pump wavelength we can find a solution for Λ and φ . Therefore noncollinear interactions can be used with tunable laser systems over an extremely broad spectral range. For comparison, a collinear configuration for generating TH is possible only at one discrete fundamental wavelength of 3561 nm.⁸ The use of first-order QPM vectors ($m_1=m_2=1$) allows us to extract the maximum efficiency and is very tolerant to duty cycle errors.

Figure 2 illustrates the experimental setup used to enable the THG DPM process. An optical parametric oscillator (OPO), pumped by a 1047 nm Q-switched Nd:YLF laser, was used to generate signal and idler waves at the desired wavelengths. The OPO consisted of a 50 mm long periodically poled LiNbO₃ (PPLN) crystal with a 29.5 μm period, held in a temperature-controlled oven inside a plano-convex cavity. The OPO temperature was varied between 100°C and 200°C to produce an idler wave of varying wavelength between 3307 and 2977 nm. The signal wave was filtered out with a 4 mm Ge plate, positioned at the Brewster angle. The frequency tripler was a 10 mm \times 7 mm \times 0.5 mm PPLN crystal with an 8 μm period, held in a temperature-controlled rotating stage with an angular resolution of 0.016°. An IR transmitting lens focused the pump wave to the crystal with a waist of $\sim 70 \mu\text{m}$.

We have achieved DPM and generated 2ω and 3ω signals at internal angles of $\sim 5.2^\circ$ and $\sim 6.9^\circ$ with respect to the fundamental. The 2ω and 3ω wavelengths were measured by an ANDO AQ6317B optical spectrum analyzer.

All experimental results were compared with a numerical simulation, in which the input was a nondepleted single-mode Gaussian beam having a waist of 70 μm in the middle of the crystal. The nonlinear polarization induced by this beam in a perfectly poled PPLN crystal was used as a source for generating the SH. A beam-propagation approach was used. We divided the crystals into slabs of 2 μm thickness and convolved in each slab the generated source with the impulse response of a free-space slab. For calculating the TH, the same method was used, but this time the nonlinear polarization was the product of the pump wave and the generated SH wave.

We measured the temperature tuning curves for the generated 2ω and 3ω waves at a fixed pump wavelength. The pump wavelength was chosen to impose double-resonance conditions for the 2ω and 3ω waves, i.e., the wavelength for which the same crys-

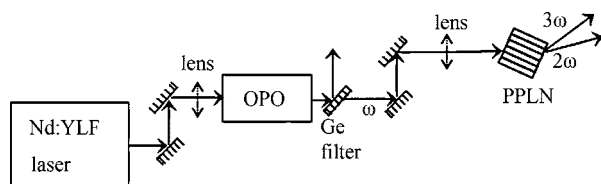


Fig. 2. Experimental setup for simultaneous generation of SH and TH of the OPO idler wave ω .

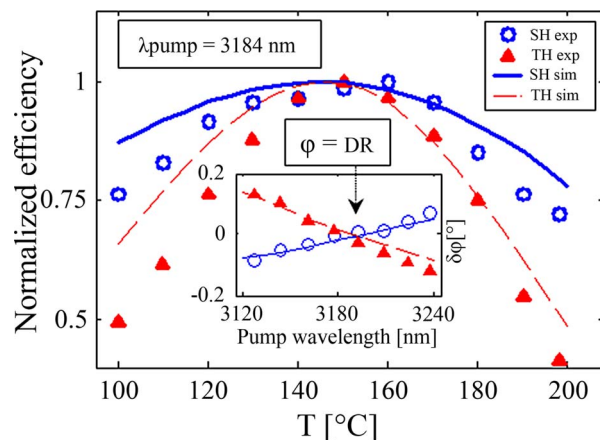


Fig. 3. (Color online) Temperature tuning curves for 2ω (open circles, experimental; solid curve, simulation) and 3ω (triangles, experimental; dashed curve, simulation) at the double-resonance (DR) point shown in the inset. Inset, double-resonance point for the SHG and THG processes for $T=150^\circ\text{C}$. For every pump wavelength the crystal angle configuration that produces peak powers for 2ω and 3ω is measured. The intersection is the double-resonance point.

tal's angle configuration gives maximum power for both waves, as shown in the inset of Fig. 3. Note that the angular tolerance for the double-resonance point is relatively tight, $<0.1^\circ$. At the pump wavelength that satisfies this double-resonance condition, we observed a fairly broad full width at half-maximum (FWHM) of $\sim 160^\circ\text{C}$ for the SHG process and $\sim 90^\circ\text{C}$ for the THG process, as shown in Fig. 3. Each efficiency curve is normalized to its own peak efficiency value. For both the SH and TH waves the simulation and the experiment show similar curves with matching peaks, although the simulation curve widths are somewhat wider than the experimental widths.

We also measured the wavelength and angle tuning curves for the generated SH and TH waves. For wavelength tuning measurements, we fixed the crystal temperature to 150°C and set the crystal angle near the double-resonance angle. We then changed the pump wavelength by changing the OPO crystal temperature and measured the powers for the pump and the generated waves. Figure 4(a) shows the conversion efficiency as a function of pump wavelength, normalized to the respective peak efficiency value. The experimental wavelength FWHM for the SH and TH waves are ~ 300 and ~ 75 nm, respectively. The SH peak was observed at 3110 nm, and the TH peak was measured at 3178 nm. The small difference between these two peaks may be caused by operating at an angle that is slightly different from the double resonance point. The theoretical curve of Fig. 4(a) was calculated at an angle that is different by $\sim 0.03^\circ$ (at a pump wavelength of 3184 nm) from the double-resonance condition.

To measure the angle tuning, the crystal temperature and pump wavelength were set to 150°C and 3184 nm, respectively. We rotated the stage and measured the powers for the pump and the generated waves. The normalized efficiency tuning curves (with respect to the maximal efficiency) for the SH and TH waves are shown in Fig. 4(b). The experimental an-

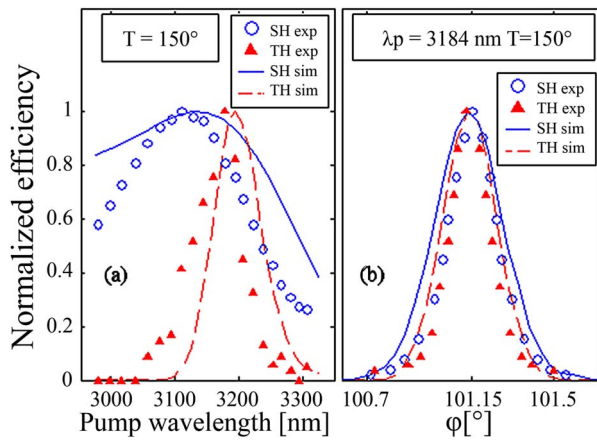


Fig. 4. (Color online) (a) Wavelength and (b) angle tuning curves for 2ω (open circles, experimental; solid curve, simulation) and 3ω (triangles, experimental; dashed curve, simulation).

gular FWHM for the SH and TH waves are 0.23° and 0.20° , respectively, which again are slightly narrower compared with the simulation.

We measured the conversion efficiencies for the generated waves at the double-resonance point, using a pump wave of 8 mW average power with a pulse width of 7 ns and repetition rate of 2.07 kHz. The SH and TH wave average powers were $51 \mu\text{W}$ and 518 nW , respectively, corresponding to internal conversion efficiencies calculated with respect to a single pulse power of $2 \times 10^{-3} \% \text{ W}^{-1}$ and $4.4 \times 10^{-8} \% \text{ W}^{-2}$, respectively. The calculated efficiencies are approximately fourfold higher, i.e., $8 \times 10^{-3} \% \text{ W}^{-1}$ for the SH and $2 \times 10^{-7} \% \text{ W}^{-2}$ for the TH. The conversion efficiency depends on the walk-off angle and is maximized for a collinear interaction. For comparison, the reported experimental SH and TH conversion efficiencies in a collinear interaction based on coincidence⁸ or on quasi-periodic structure⁴ are $5.4 \times 10^{-2} \% \text{ W}^{-1}$ ($10^{-4} \% \text{ W}^{-2}$) and $4.9 \times 10^{-2} \% \text{ W}^{-1}$ ($3 \times 10^{-5} \% \text{ W}^{-2}$), respectively.

The differences between the experimental results and the calculation may be caused by having an experimental pump wave with a spectral width of $\sim 6 \text{ nm}$ (while assuming a monochromatic wave in the simulation), possible deviations of this pump wave from a perfect Gaussian beam, and imperfection in the poling pattern of the PPLN. Nevertheless, the experimental results agree reasonably well with the simulation, in the thermal, angular, and spectral performance, as well as in the conversion efficiencies.

The THG is just one of many implementations that noncollinear DPM process can be used for. For example, DPM can be used for all-optical deflection by using a cascaded interaction employing the ordinary and extraordinary polarizations of the fundamental wave. The two processes that should be simultaneously phase matched are the SH of the extraordi-

nary pump and the difference frequency of the generated SH and a cross polarized (ordinary) signal wave at the same frequency, to generate a deflected signal wave. For the same $8 \mu\text{m}$ period PPLN crystal with a 3420 nm fundamental wave, incident on the crystal at $\varphi = 86^\circ$, and a choice of $m_1 = 3$, $m_2 = 1$, the nonlinear ordinary wave will be deflected by 23.4° .

In summary, we have demonstrated in this Letter THG achieved by noncollinear DPM in a 1D periodically poled crystal. The noncollinear interaction allowed the use of first-order QPM processes for achieving DPM. Furthermore, it permitted angular separation of all three output beams. The broad measured spectral tuning of the noncollinear interaction may be useful for ultrashort pulse frequency conversion. We studied the dependence of this process on various experimental parameters, including the crystal temperature, the entrance angle, and the pump wavelength and power. While this experiment was conducted with an infrared pump, the technique may be implemented at much shorter wavelengths, since submicrometer poling is now possible with ferroelectric crystals.^{10,11} In addition to multiple-harmonic generation, this technique can be also applied for all-optical processing and for other cascaded nonlinear effects.

This work was supported by the Israel Science Foundation, grant 960/05. S. M. Saltiel thanks Tel Aviv University for hospitality, the Gordon Center for Energy Studies, and Bulgarian science fund (grant F1201). A. Arie's e-mail address is ady@eng.tau.ac.il.

References

1. J. A. Armstrong, N. Bloembergen, J. Ducuing, and P. S. Pershan, *Phys. Rev.* **127**, 1918 (1962).
2. S. M. Saltiel, A. A. Sukhorukov, and Y. S. Kivshar, *Prog. Opt.* **47**, 1 (2005).
3. S. Zhu, Y. Y. Zhu, and N. B. Ming, *Science* **278**, 843 (1997).
4. K. Fradkin-Kashi, A. Arie, P. Urenski, and G. Rosenman, *Phys. Rev. Lett.* **88**, 023903 (2002).
5. M. H. Chou, K. R. Parameswaran, M. M. Fejer, and I. Brener, *Opt. Lett.* **24**, 1157 (1999).
6. N. G. R. Broderick, R. T. Bratfalean, T. M. Monro, D. J. Richardson, and C. M. de Sterke, *J. Opt. Soc. Am. B* **19**, 2263 (2002).
7. R. Lifshitz, A. Arie, and A. Bahabad, *Phys. Rev. Lett.* **95**, 133901 (2005).
8. O. Pfister, J. S. Wells, L. Hollberg, L. Zink, D. A. VanBaak, M. D. Levenson, and W. R. Bosenberg, *Opt. Lett.* **22**, 1211 (1997).
9. M. D. Levenson, O. Pfister, J. S. Wells, L. Hollberg, W. R. Bosenberg, and D. A. VanBaak, in *Nonlinear Optics '98: Materials, Fundamentals and Applications, Topical Meeting* (IEEE, 1998), pp. 180.
10. C. Canalias, V. Pasiskevicius, R. Clemens, and F. Laurell, *Appl. Phys. Lett.* **82**, 4233 (2003).
11. S. Moscovich, A. Arie, R. Urenski, A. Agronin, G. Rosenman, and Y. Rosenwaks, *Opt. Express* **12**, 2236 (2004).